nature genetics

Amplification of siRNA in *Caenorhabditis elegans* generates a transgenerational sequence-targeted histone H3 lysine 9 methylation footprint

Sam Guoping Gu[1], Julia Pak[1], Shouhong Guang[2,4], Jay M Maniar[3], Scott Kennedy[2] & Andrew Fire[1,3]

Exogenous double-stranded RNA (dsRNA) has been shown to exert homology-dependent effects at the level of both target mRNA stability and chromatin structure. Using *C. elegans* undergoing RNAi as an animal model, we have investigated the generality, scope and longevity of dsRNA-targeted chromatin effects and their dependence on components of the RNAi machinery. Using high-resolution genome-wide chromatin profiling, we found that a diverse set of genes can be induced to acquire locus-specific enrichment of histone H3 lysine 9 trimethylation (H3K9me3), with modification footprints extending several kilobases from the site of dsRNA homology and with locus specificity sufficient to distinguish the targeted locus from the other 20,000 genes in the *C. elegans* genome. Genetic analysis of the response indicated that factors responsible for secondary siRNA production during RNAi were required for effective targeting of chromatin. Temporal analysis revealed that H3K9me3, once triggered by dsRNA, can be maintained in the absence of dsRNA for at least two generations before being lost. These results implicate dsRNA-triggered chromatin modification in *C. elegans* as a programmable and locus-specific response defining a metastable state that can persist through generational boundaries.

RNA interference (RNAi) is defined as the ability of exogenous dsRNA to silence homologous target genes[1,2]. The RNAi pathway begins with dsRNA being diced into small RNAs of 20–30 nucleotides (known as small interfering RNAs or siRNAs) by the RNase III–like enzyme dicer[3]. siRNAs are then loaded onto highly conserved argonaute proteins, defined by an RNaseH-like 'PIWI' domain and an RNA-coordinating 'PAZ' domain[4]. Target mRNAs are recognized by siRNA-mediated base-pairing interactions and are degraded by the nuclease ('slicer') activity of some argonautes[5–7]. In plants, fungi and *C. elegans*, dicer-produced siRNA (primary siRNA) can also trigger *de novo* synthesis of additional small RNA (secondary siRNA) through recruitment of RNA-directed RNA polymerases (RdRPs) that use the mature target mRNA as a template[8–10]. Endogenous small RNAs that are antisense to transcripts also exist in a variety of eukaryotic species. These endo-siRNAs modulate a diverse set of cellular processes, such as gene regulation, genome surveillance and chromosome transmission[11–15].

In addition to mRNA degradation, RNA-mediated alterations have also been described at the DNA or chromatin level[16,17]. These modifications occur in a process termed 'RNA-triggered chromatin modification' that is distinct from cytoplasmic RNA-triggered mRNA degradation mechanisms that are referred to as RNAi. RNA-triggered chromatin modification was initially discovered in plants, where it was found that transgene or viral RNA can trigger a local peak of DNA methylation around the target sequence[18,19]. RNA-mediated DNA methylation in plants involves small RNAs and requires dicer, argonaute and RdRP family members. In *Schizosaccharomyces pombe*, endogenous small RNAs derived from DNA repeats are associated with heterochromatic gene silencing at the pericentromeric and subtelomeric regions and at the mating type locus[20–22]. At these heterochromatic loci, RNAi factors (argonaute protein Ago1, dicer protein Dcr1 and RNA-dependent RNA polymerase Rdp1) participate in direct interactions with heterochomatin-associated proteins (for example, chromodomain protein Chp1), with these interactions being required for H3K9me3, a histone posttranslational modification associated with silenced chromatin[23–26]. In some cases, exogenous dsRNA was sufficient to direct defined chromatin modifications in *S. pombe*[27–30]. In an analogous situation, siRNA-mediated chromatin changes may serve as a basis for genome rearrangements during macronuclear development in *Tetrahymena*, where siRNA populations have been shown to induce a localized alteration in chromatin that becomes evident after later genome rearrangement[31–33].

Indications of siRNA-chromatin associations in animal systems initially came from indirect experiments. One set of observations describe defects in heterochromatin formation at centromeric regions in *Drosophila* and mouse germ cells affected by mutations in RNAi components[34–36]. Although such results outline some type of link between RNA triggers and chromatin modification, the existence of

[1]Department of Pathology, Stanford University School of Medicine, Stanford, California, USA. [2]Laboratory of Genetics, University of Wisconsin–Madison, Madison, Wisconsin, USA. [3]Department of Genetics, Stanford University School of Medicine, Stanford, California, USA. [4]Current address: School of Life Sciences, University of Science & Technology of China, Hefei, China. Correspondence should be addressed to A.F. (afire@stanford.edu).

Received 17 August 2011; accepted 17 November 2011; published online 8 January 2012; doi:10.1038/ng.1039

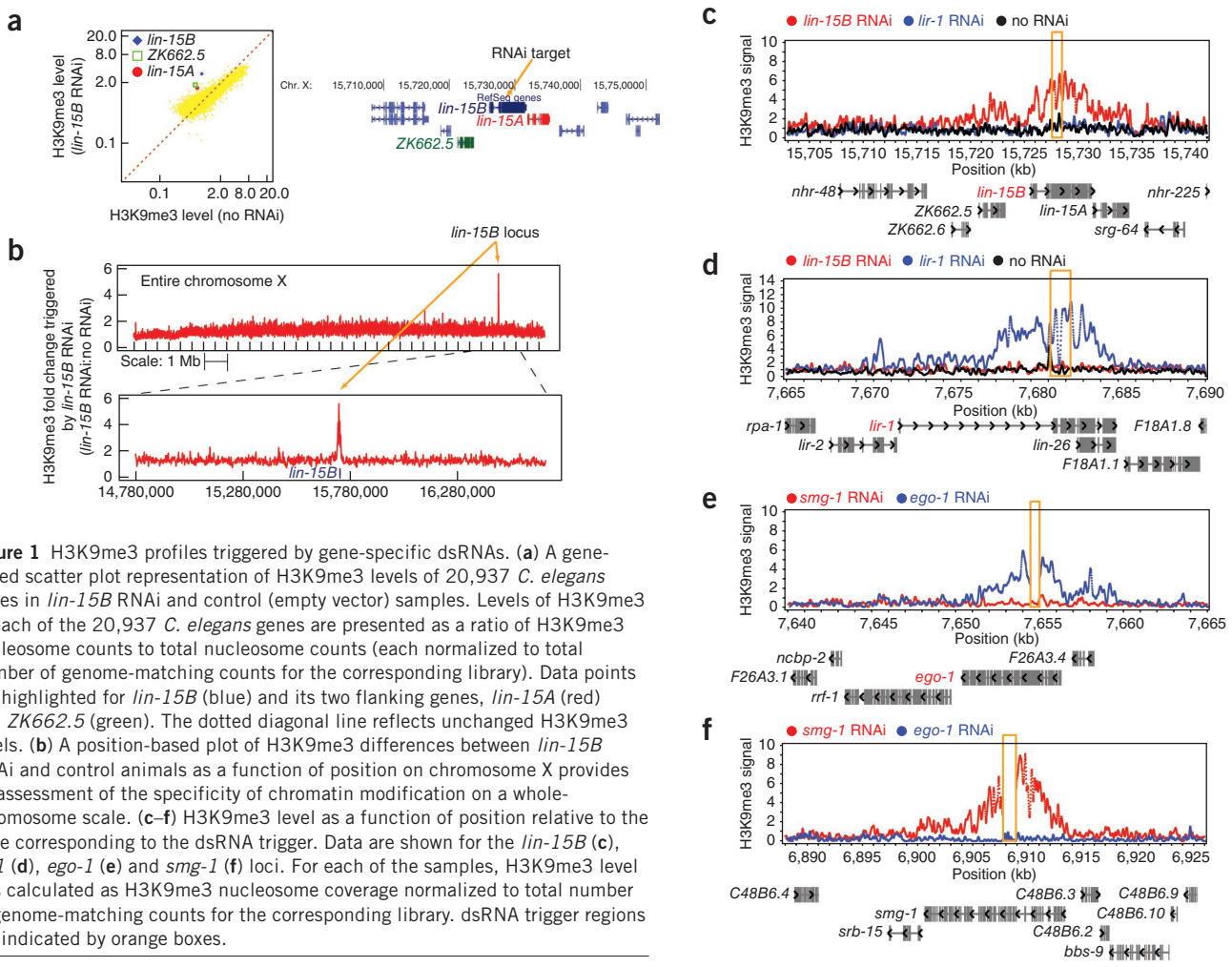

Figure 1 H3K9me3 profiles triggered by gene-specific dsRNAs. (**a**) A gene-based scatter plot representation of H3K9me3 levels of 20,937 *C. elegans* genes in *lin-15B* RNAi and control (empty vector) samples. Levels of H3K9me3 at each of the 20,937 *C. elegans* genes are presented as a ratio of H3K9me3 nucleosome counts to total nucleosome counts (each normalized to total number of genome-matching counts for the corresponding library). Data points are highlighted for *lin-15B* (blue) and its two flanking genes, *lin-15A* (red) and *ZK662.5* (green). The dotted diagonal line reflects unchanged H3K9me3 levels. (**b**) A position-based plot of H3K9me3 differences between *lin-15B* RNAi and control animals as a function of position on chromosome X provides an assessment of the specificity of chromatin modification on a whole-chromosome scale. (**c**–**f**) H3K9me3 level as a function of position relative to the gene corresponding to the dsRNA trigger. Data are shown for the *lin-15B* (**c**), *lir-1* (**d**), *ego-1* (**e**) and *smg-1* (**f**) loci. For each of the samples, H3K9me3 level was calculated as H3K9me3 nucleosome coverage normalized to total number of genome-matching counts for the corresponding library. dsRNA trigger regions are indicated by orange boxes.

global chromatin defects in mutant strains lacking RNAi components is not *prima facie* evidence for homology-targeted chromatin modification (rather, some of these defects could be secondary to other major defects in cellular metabolism in the global absence of functional RNA-based regulation). Adding to this debate, various studies in mammalian cell culture systems have described a combination of sequence-specific and sequence-nonspecific responses to foreign dsRNA[34–38]. The variety of results in such assays illustrates both the real potential for diverse responses to siRNA in clinically important systems and the need for model systems to analyze these changes using tractable organisms and genomes[39–41].

Several features make *C. elegans* an attractive animal model to study chromatin-targeted RNA effects. dsRNA can be conveniently introduced to the animals by microinjection, feeding or soaking[1,42,43], with each mode of administration sufficient to produce substantial effects on target gene expression. A large number of genes can be silenced in *C. elegans*, thus allowing a wide variety of activity assays. *C. elegans* appears to share the ability to respond to dsRNA at both the RNA and chromatin levels[44–46]. Early studies in *C. elegans* found reduced levels of target mRNA in both the cytoplasm and nucleus of dsRNA-treated embryos[46], with the potential for both specific and nonspecific responses to dsRNA at the chromatin level[47]. Recent studies have focused on specific assays for a number of loci and have identified a set of nuclear RNAi-defective (nrde) genes (for example, *nrde-2* and *nrde-3*) whose functions are required for nucleus-based gene silencing[44,45]. Specificity and generality have been extensively studied for cytoplasmic RNAi, but these issues have remained something of a mystery in dsRNA-triggered chromatin modification. In this work, we make use of high-throughput chromatin structure assays to assess the specificity of the effects of chromatin-targeted dsRNA and to characterize the relationship between classical (cytoplasmic) RNAi and RNA-triggered chromatin modification.

RESULTS

Specificity of RNA-triggered chromatin effects in *C. elegans*

We first examined the specificity of dsRNA-triggered H3K9me3 modification by targeting the *lin-15B* gene, which was a model substrate in previous analyses of the nuclear effects of RNAi in *C. elegans*[44,45]. A genome-wide assessment of RNAi effects was performed using chromatin immunoprecipitation (ChIP) of nucleosome core particles[48] followed by high-throughput sequencing (ChIP-Seq) (**Fig. 1**). As a number of studies of nuclear RNAi have used *eri-1*(*mg366*) as a dsRNA-recipient strain ('eri' signifies enhanced RNAi[49]), we carried out our initial analysis in synchronized embryos of this genetic background.

An initial examination of target specificity was performed by comparing the degree of H3K9me3 modification for each gene in animals with RNA interference for *lin-15B* and in control animals (**Fig. 1a**). Counts from nucleosome cores isolated by H3K9me3

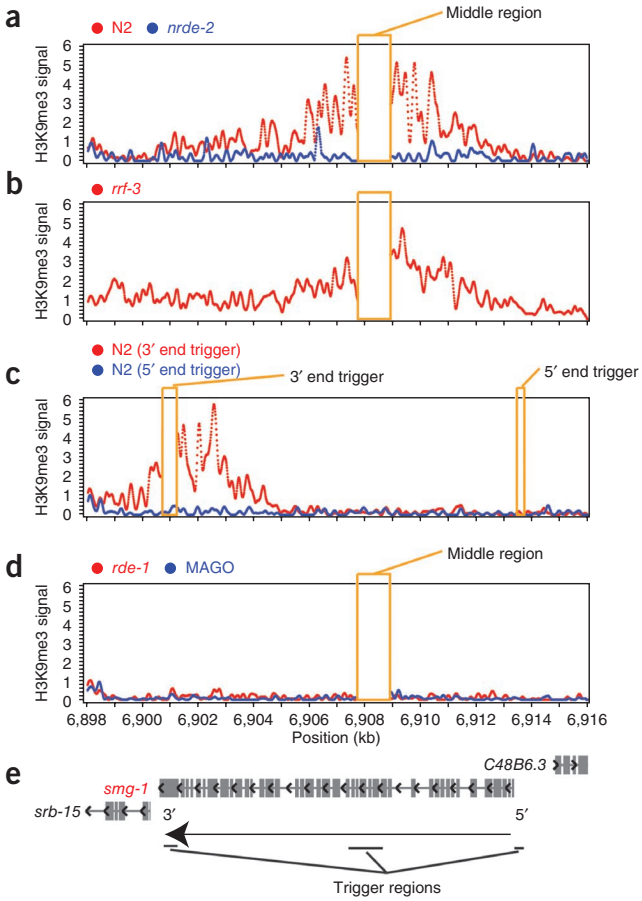

Figure 2 H3K9me3 profiles triggered by dsRNAs that target different sections of the *smg-1* locus. (**a**–**d**) dsRNA targeting the middle section (**a**,**b**,**d**), 3′ UTR (**c**, red line) or a region upstream of the 5′ end of *smg-1* mRNA (**c**, blue line). Trigger regions are indicated by orange boxes, and the genetic backgrounds are specified. The H3K9me3 profile generated from the *nrde-2* mutant (*smg-1* RNAi) represents a baseline of H3K9me3 modification in the absence of a functional RNAi pathway. (**e**) Map of the *smg-1* locus.

immunoprecipitation were normalized using counts from nucleosome cores isolated without immunoprecipitation. Among the 20,937 *C. elegans* genes surveyed for this analysis, *lin-15B* showed the highest increase in dsRNA-triggered H3K9me3. Two genes (*lin-15A* and *ZK662.5*) that are located next to *lin-15B* in the genome also showed increased H3K9me3 levels in the *lin-15B* RNAi animals. Most of the other genes remained distributed along the diagonal line in the scatter plot, indicating little if any change in H3K9 trimethylation in those targets with *lin-15B* RNAi. Another analysis of target specificity was carried out by comparing the degree of H3K9me3 modification across the entire X chromosome (using a 2-kb smoothing window) in animals with RNA interference for *lin-15B* and in control animals (**Fig. 1b**). The biggest difference in H3K9me3 levels occurred in the *lin-15B* region (5.7-fold enrichment). These data indicate that the strong H3K9me3 enhancement following *lin-15B* RNAi was specific to the *lin-15B* region and neighboring loci.

A detailed local analysis showed the extent of spreading in the eventual distribution of H3K9me3 after dsRNA administration (**Fig. 1c**). The highest H3K9me3 levels were seen in the trigger region and its flanking sequences (on average, the H3K9me3 level at the trigger region was 3.7 times the background level). Using a cutoff of a twofold change above the background H3K9me3 level, we found that H3K9me3 could spread as far as 9 kb from the trigger region.

Susceptibility of diverse loci to RNA-triggered modification

We chose three other target genes (*lir-1*, *ego-1* and *smg-1*) for RNAi in the *eri-1*(*mg366*) mutant background. Because *lir-1* is abundantly expressed in embryos[50], we induced *lir-1* RNAi in animals and collected embryos for H3K9me3 profiling (**Fig. 1d**). Both *smg-1* and *ego-1* function in germline cells (*smg-1* functions in the somatic cells as well)[51,52]. Therefore, for *smg-1* and *ego-1* RNAi experiments, synchronized adult animals were used (**Fig. 1e**,**f**).

In control animals not exposed to specific RNAi, the *lir-1*, *ego-1* and *smg-1* loci had very low levels of H3K9me3. In the RNAi animals, we observed a dramatic accumulation of H3K9me3, with strong specificity for the target gene in each case (**Fig. 1d**–**f**). These data suggest that many genes in *C. elegans* are susceptible to dsRNA-triggered chromatin modification.

As with *lin-15B* RNAi, we observed a distinctive spatial pattern of dsRNA-triggered chromatin modification for the tested target loci. In each case, the highest levels of H3K9me3 accumulation occurred at the trigger region or in the immediate flanking sequences (**Fig. 1d**–**f**). The H3K9me3 profiles within the trigger regions were excluded for the *smg-1* and *ego-1* RNAi experiments because DNA fragments from RNAi feeding plasmids were captured and amplified in immunoprecipitated material (**Fig. 1e**,**f**). In contrast, embryos were free from contaminating feeding vector DNA because of a hypochlorite washing step[53] that removed bacteria during embryo preparation (**Fig. 1c**,**d**), allowing H3K9me3 profiling in these animals. Using a cutoff of a twofold change above the background H3K9me3 level, we found that the H3K9me3 modification could spread as far as 11, 6 and 8 kb from the trigger regions of *lir-1*, *ego-1* and *smg-1*, respectively. In all cases, the H3K9me3 spread into intergenic regions and some of the neighboring genes. These data indicate that the spread of chromatin modifications over a distance from the trigger region equivalent to several gene lengths is a common feature of dsRNA-triggered chromatin modification.

RNA-triggered chromatin modification in wild-type animals

Guang *et al.* have shown that RNAi-enhancing mutations are required at some targets for efficient induction of phenotypes through nuclear pathways[45]. Similarly, effective chromatin responses to exogenous dsRNA in *S. pombe* have been reported in a subset of studies to require mutations in analogous genes[27,28].

To test whether sensitizing mutations in the *eri* pathway were required for the chromatin response, we compared H3K9me3 levels in the *eri-1*(*mg366*) and wild-type (strain N2) genetic backgrounds. This analysis was carried out using the *smg-1* target locus. In these experiments, we observed an increase in H3K9me3 at the target gene in the wild-type animals in response to *smg-1* dsRNA (**Fig. 2a**), with only a modest decrease in the degree of enrichment for H3K9me3 and the extent of H3K9me3 spreading relative to the *eri-1* genetic background. As a control to ensure our ability to detect defects in dsRNA-triggered H3K9me3 modification in this assay, we measured modification in an *nrde-2*(*gg091*) genetic background previously shown to compromise chromatin-targeted RNAi. *nrde-2* mutant animals showed a 6× decrease in H3K9me3 in response to dsRNA compared with the *eri-1* and wild-type strains, thereby showing the specificity of the ChIP-Seq assay (**Fig. 2a**). These data indicate that the chromatin response is not dependent on the *eri-1* mutation. Similar results were obtained with the RNAi-enhancing mutation in the *rrf-3*(*pk1426*) strain (**Fig. 2b**).

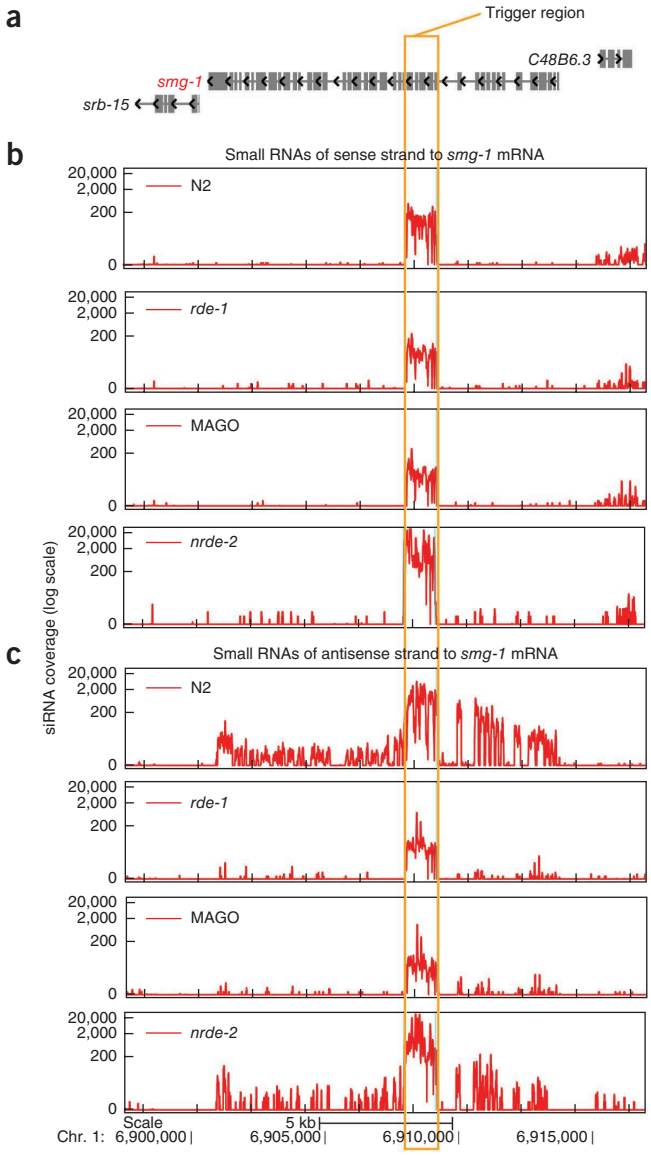

Figure 3 Small RNA coverage profiles at the *smg-1* locus after exposure to *smg-1* dsRNA in various genetic backgrounds. (**a**) Map of the *smg-1* locus. (**b**,**c**) Coverages for small RNAs that matched the *smg-1* mRNA sense strand (**b**) or the *smg-1* mRNA antisense strand (**c**) were plotted separately. The level of small RNAs was normalized by the total number (in millions) of small RNAs that matched the reverse complement sequences of total *C. elegans* mRNAs. Trigger regions are indicated by orange boxes, and the genetic backgrounds are specified.

The chromatin response to dsRNA as a subgenic effect

To investigate the relationship between the dsRNA trigger and the position of dsRNA-mediated chromatin modification, we examined the effect of an *smg-1* RNAi trigger targeting the 3′ untranslated region (UTR) of this gene (**Fig. 2c**). We found that this 7-kb downstream shift in the trigger location was accompanied by a 7-kb shift in the H3K9me3 peak center (compare red traces in **Fig. 2a** and **Fig. 2c**). The spatial correlation between the triggering dsRNA and H3K9me3 profile reveals a mechanism in which the specificity of the chromatin response is determined by events on a subgenic scale.

No methylation signal was observed when using dsRNA targeting a region upstream of the annotated *smg-1* 5′ UTR (**Fig. 2c**, blue trace). This observation is consistent with models in which interactions with a pool of target mRNAs might have an essential role in the eventual targeting of chromatin. Several other observations, noted below, support this type of model.

Requirement for secondary siRNA argonautes

Primary and secondary siRNAs in *C. elegans* are two classes of small RNAs that differ in their biogenesis, chemical structure at the 5′ end and strand specificity. Primary siRNAs are cleaved from the initial dsRNA trigger by dicer, are derived from both strands and carry a 5′-monophosphate terminus. Secondary siRNAs are produced through the primary siRNA–guided action of RNA-directed RNA polymerases on specific mRNA templates, resulting in the production of large numbers of short antisense transcripts that retain triphosphate on their 5′ end. Two groups of argonaute proteins participate in classical RNAi in *C. elegans*: RDE-1 incorporates primary siRNAs and mediates interactions of the primary siRNAs with target templates, resulting in recruitment of RdRP activities[9,10,54,55], and a group of additional argonautes (PIWI-1, SAGO-1, SAGO-2 and F58G1.1) then interact with secondary siRNAs, presumably allowing additional target mRNAs to be detected and cleared[56].

To investigate the participation of different small RNA classes and their corresponding argonuate factors in chromatin-targeted RNAi, we examined small RNA profiles and argonaute genetic requirements for this process. *smg-1* RNAi experiments were carried out in populations of *C. elegans* mutant for either *rde-1* (*rde-1*(*ne300*)) or the secondary argonaute group (MAGO (*ppw-1*(*tm914*), *sago-1* (*tm1195*), *sago-2*(*tm894*), *F58G1.1*(*tm1019*), *C06A1.4*(*tm887*) and *M03D4.6*(*tm1144*)). Neither population of mutant animals showed H3K9me3 accumulation above background levels at the target locus (**Fig. 2d**,**e**), suggesting that the two sets of argonautes are both essential for the dsRNA-triggered chromatin response.

In order to correlate chromatin responses with small RNA populations, we also examined the small RNA profiles in the RNAi mutant worms by using a 5′-monophosphate–independent small RNA cloning method, which captures both the primary (5′-monophosphate) and the secondary (5′-triphosphate) siRNAs. RNAi in the wild-type sample produced a large number of small RNAs. In *rde-1*(*ne300*) and MAGO mutants, the numbers of primary siRNAs at the trigger region was reduced only by a factor of 3–4× relative to the wild-type animals (**Fig. 3a**,**b**). In contrast, secondary siRNA levels at the *smg-1* locus in *rde-1*(*ne300*) and MAGO mutants were reduced by 360 and 197 fold, respectively, compared to wild-type animals (**Fig. 3c**).

Secondary siRNA accumulation alone did not seem to be sufficient for a robust chromosomal effect following *smg-1* RNAi. As *nrde-2* (*gg091*) mutant animals, which lack a chromatin-targeted H3K9me3 response, retained the ability to make secondary as well as primary siRNAs (**Fig. 3b**,**c**), it is evident that there is at least one additional mechanistic requirement in this process. Somewhat surprisingly, siRNA counts in *nrde-2*(*gg091*) mutants seemed to be higher than in wild-type animals, which could indicate a global readjustment of specific small RNA dynamics in the *nrde-2*(*gg091*) strain (such as increased *in vivo* stability of siRNAs incorporated into alternative argonautes). Taken together, these data are consistent with a mechanism for dsRNA-triggered chromatin modification that depends on (but also extends to) the dsRNA-triggered secondary siRNA response.

Multigenerational character of the chromatin response

Previous studies have shown that dsRNA-triggered gene silencing effects can last for multiple generations in *C. elegans*[55,57,58]. Such heritable

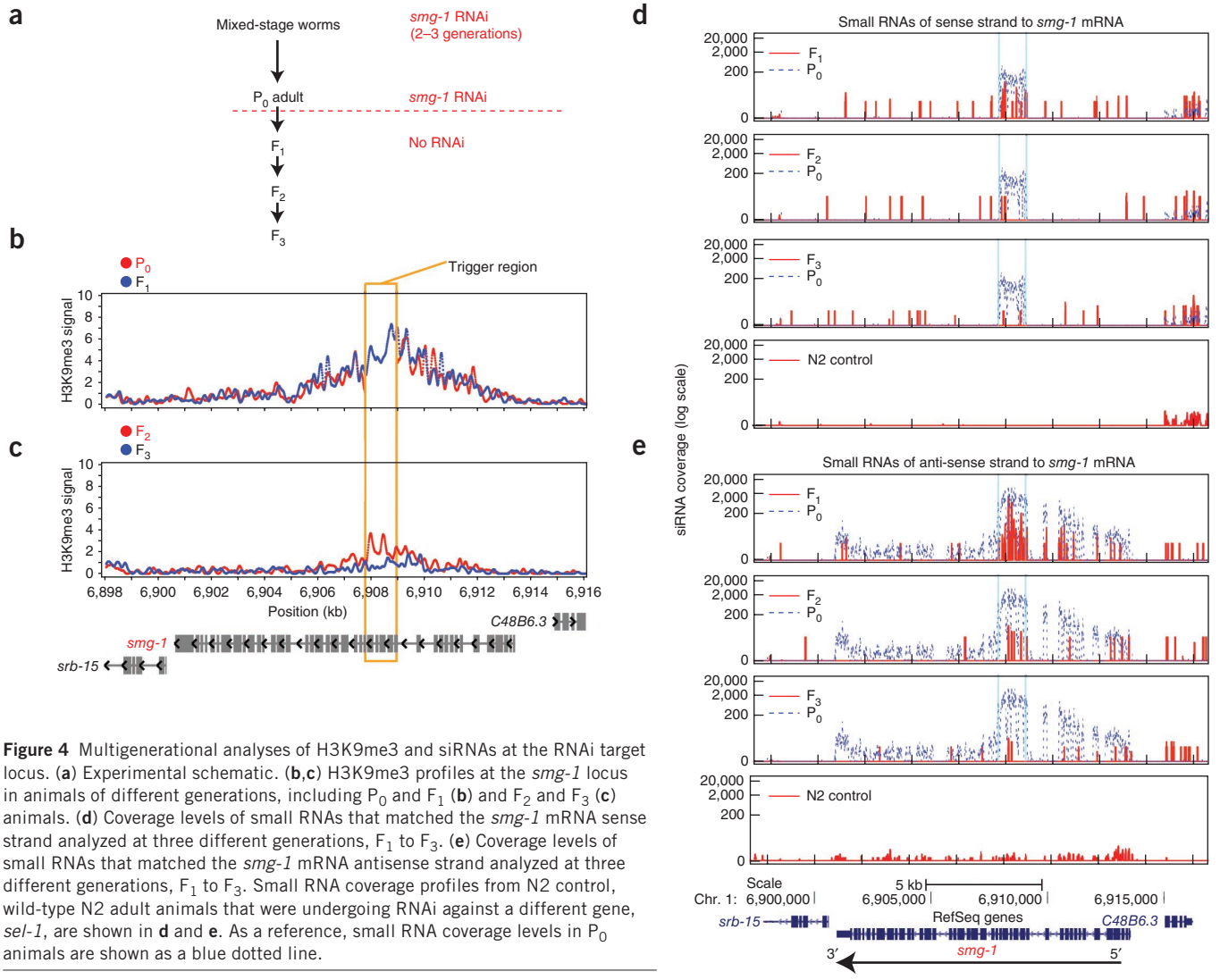

Figure 4 Multigenerational analyses of H3K9me3 and siRNAs at the RNAi target locus. (**a**) Experimental schematic. (**b**,**c**) H3K9me3 profiles at the *smg-1* locus in animals of different generations, including P_0 and F_1 (**b**) and F_2 and F_3 (**c**) animals. (**d**) Coverage levels of small RNAs that matched the *smg-1* mRNA sense strand analyzed at three different generations, F_1 to F_3. (**e**) Coverage levels of small RNAs that matched the *smg-1* mRNA antisense strand analyzed at three different generations, F_1 to F_3. Small RNA coverage profiles from N2 control, wild-type N2 adult animals that were undergoing RNAi against a different gene, *sel-1*, are shown in **d** and **e**. As a reference, small RNA coverage levels in P_0 animals are shown as a blue dotted line.

silencing effects could conceivably have been mediated by small RNA–directed or chromatin-based mechanisms (or a combination of effects). Here, we investigated whether the heterochromatin state and/or siRNAs at the RNAi target gene can be maintained for subsequent generations in the absence of continued exposure to the initial dsRNA trigger. To address this question, we profiled H3K9me3 and siRNA levels in the progeny of *smg-1* RNAi worms for multiple generations (**Fig. 4** and Online Methods). Wild-type adult animals were exposed to *smg-1* RNAi for 2–3 generations and subsequently bleached to produce a synchronized population, which was again exposed to *smg-1* RNAi. A subset of adult animals was harvested (the P_0 generation), and we then removed the dsRNA source and collected F_1, F_2 and F_3 populations at the adult stage. All animals were processed for small RNA and H3K9me3 profiling. We observed that the magnitude and spread of the H3K9me3 modification in the F_1 animals were at levels similar to those in the P_0 animals (**Fig. 4b**). Of note, the siRNA level in the F_1 adult animals was much lower than in P_0 worms that had been directly exposed to *smg-1* dsRNA (depletion for primary and secondary siRNAs to 0.24% and 0.14%, respectively) (**Fig. 4d** compared with **Fig. 3b** and **Fig. 4e** compared with **Fig. 3c**, respectively). The chromatin response weakened in F_2 animals but was still distinctively present (**Fig. 4c**). In F_3 animals, H3K9me3 levels reverted to near background (**Fig. 4c**; H3K9me3 signals at the *smg-1* locus (2-kb windows flanking the trigger site) from P_0, F_1, F_2 and F_3 populations were 8.3, 9.2, 3.7 and 1.6 times the background level seen in *smg-1* RNAi *nrde-2*(*gg091*) mutant animals). These results indicate that the H3K9me3 response, once established at the RNAi target gene, can persist for at least two generations without any further dsRNA exposure. The persistence could reflect either a very potent biological activity of the residual low levels of trigger RNA found in the progeny generations or a maintenance of the modified chromatin in the absence of an RNA requirement.

Time lag between siRNA accumulation and chromatin response

Previous study has shown that exogenous dsRNA-triggered siRNAs could engage in the RNAi pathway within a few hours of their introduction[46,56]. Here, we investigated the time lag between dsRNA exposure and chromatin response. We performed two time-course experiments in which worms were harvested 4 or 24 h after synchronized larvae started to feed on bacteria expressing *smg-1* dsRNA (see **Fig. 5** for a schematic). L4 larvae were harvested from each experiment for small RNA and H3K9me3 profiling to provide populations of both somatic and germline tissues. We observed a high level of *smg-1* siRNA at the 4-h time point, with even higher *smg-1* siRNA levels at

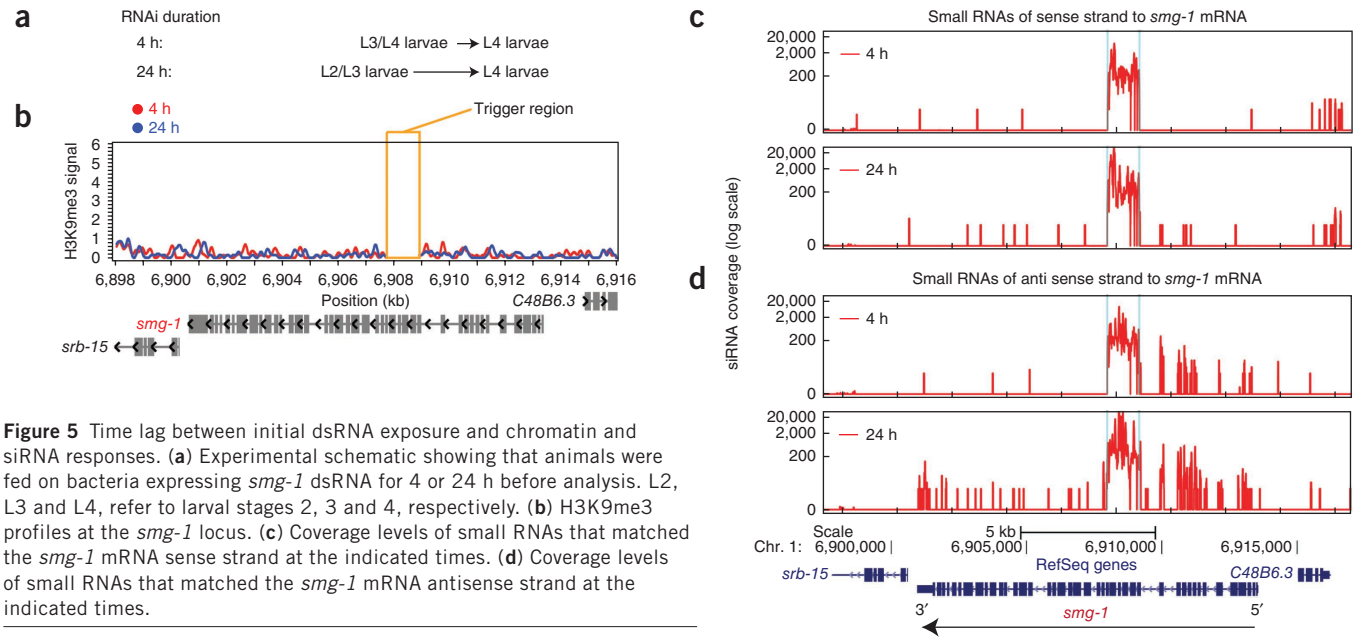

Figure 5 Time lag between initial dsRNA exposure and chromatin and siRNA responses. (**a**) Experimental schematic showing that animals were fed on bacteria expressing *smg-1* dsRNA for 4 or 24 h before analysis. L2, L3 and L4, refer to larval stages 2, 3 and 4, respectively. (**b**) H3K9me3 profiles at the *smg-1* locus. (**c**) Coverage levels of small RNAs that matched the *smg-1* mRNA sense strand at the indicated times. (**d**) Coverage levels of small RNAs that matched the *smg-1* mRNA antisense strand at the indicated times.

the 24-h time point (**Fig. 5c**), indicating an ongoing RNAi process. In contrast, we did not observe any accumulation of H3K9me3 at the *smg-1* locus at either 4 or 24 h after RNAi induction (**Fig. 5b**). These data indicate that, in addition to being required for H3K9 methylation, siRNA accumulation precedes this modification. Moreover, we suggest that distinct and separable mechanisms mediate these events.

DISCUSSION

We have described several features and genetic requirements for dsRNA-triggered chromatin modification in *C. elegans*, with our results showing that (i) the chromatin response can be highly specific in triggering a window of H3K9me3 surrounding genomic sequences corresponding to a triggering dsRNA, (ii) the chromatin response can be targeted to many *C. elegans* genes, (iii) secondary siRNA produced through an initial interaction with an mRNA product are associated with and apparently integral to the chromatin response, (iv) in time-course experiments, dsRNA-triggered chromatin modification lags behind the initial siRNA response and (v) chromatin changes can outlast the major small RNA pools, yielding heritable effects. This work differs from a number of important previous studies[39–41,44,45] in that we have shown a direct and highly specific relationship between the dsRNA sequences introduced into the system and the targeted modification of the corresponding chromosomal region. This work draws a clear analogy to well-studied RNA-triggered chromatin modification systems originally described in plants[16–18,59] and more recently in fungi[27].

The requirement for *rde-1* and MAGO genes in dsRNA-triggered chromatin modification strongly suggests that secondary siRNAs represent a link between cytoplasmic and nuclear dsRNA responses. In particular, primary siRNA production is apparently not sufficient to trigger chromatin modification. The strong spatial correlation between dsRNA-triggered H3K9me3 and the triggering dsRNA is consistent with a model in which the secondary siRNAs (likely in an argonaute-dependent manner) directly target the nascent transcript (or even DNA) for chromatin modification.

A role for secondary siRNA machinery in the triggering of nuclear events is apparently conserved rather widely, at least in lower eukaryotes. In particular, we note the requirement for RdRP homologs in transgene RNA–directed DNA methylation in *Arabidopsis thaliana* and in site-specific hairpin-induced heterochromatin formation in *S. pombe*[29,30,60,61] In both cases an initial aberrant RNA trigger seems to be insufficient for site-specific chromatin modification, which

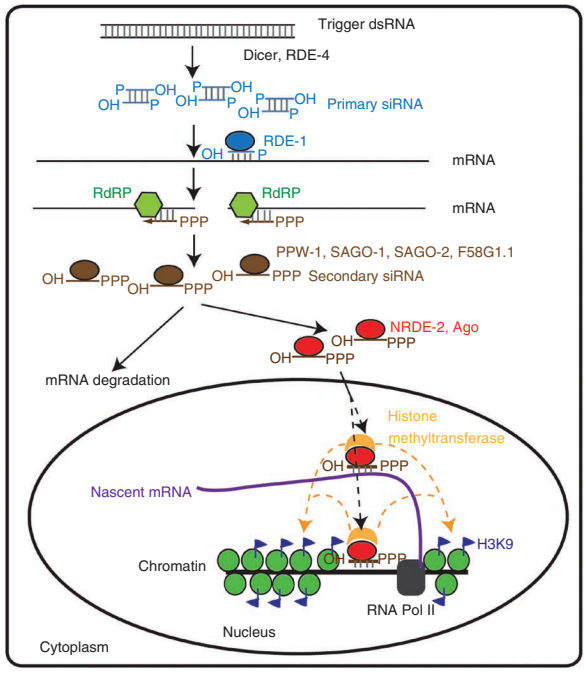

Figure 6 A working model for dsRNA-triggered H3K9 methylation in *C. elegans*. The dsRNA trigger dsRNA is digested to primary siRNAs through the activity of DICER[3] and RDE-4 (ref. 62). Primary siRNAs then incorporate into complexes with the RDE-1 argonaute[63], causing recruitment of RdRP activities (EGO-1 (ref. 51) and RRF-1 (ref. 54)). Secondary siRNAs resulting from RdRP activity incorporate into complexes with a second group of argonautes[56], including NRDE-2 (ref. 46). Targeted binding of siRNA:NRDE-2 complexes to nascent transcripts on the chromosome is proposed to recruit (directly or indirectly) one or more histone modifying components, eventually leading to H3K9 methyltransferase recruitment and the observed H3K9 modification.

Table 1 Description of libraries used for this study

Library name	Experiment description	Type of library	Genetic background	dsRNA target site	Effective reads analyzed[a]
SG0910_4lib	*ego-1* RNAi	H3K9me3 IP nucleosome	*eri-1*(*mg366*)	Chr. I:7,655,024–7,654,481 (*ego-1*)	7,458,471
SG0910_6lib	*smg-1* RNAi	H3K9me3 IP nucleosome	*eri-1*(*mg366*)	Chr. I:6,907,993–6,909,159 (*smg-1*)	11,363,856
V74_7IPmix_CAT	*lin-15B* RNAi	H3K9me3 IP nucleosome	*eri-1*(*mg366*)	Chr. X:15,728,059–15,728,991 (*lin-15B*)	11,626,719
SG0810_15lib	*lir-1* RNAi	H3K9me3 IP nucleosome	*eri-1*(*mg366*)	Chr. II:7,680,827–7,682,011 (*lir-1*)	22,575,828
V74_7IPmix_ACG	Control, no RNAi	H3K9me3 IP nucleosome	*eri-1*(*mg366*)		10,275,693
SG0411_lib54	*smg-1* RNAi (targeting the 3′ end)	H3K9me3 IP nucleosome	N2	Chr. I:6,901,030–6,901,541 (*smg-1*)	7,186,203
SG0411_lib52	*smg-1* RNAi (targeting the 5′ end)	H3K9me3 IP nucleosome	N2	Chr. I:6,913,664–6,913,933 (*smg-1*)	9,066,039
SG0411_lib20	*smg-1* RNAi	H3K9me3 IP nucleosome	N2	Chr. I:6,907,993–6,909,159 (*smg-1*)	7,748,563
SG0411_lib61	*smg-1* RNAi	H3K9me3 IP nucleosome	*nrde2*(*gg091*)	Chr. I:6,907,993–6,909,159 (*smg-1*)	5,342,704
SG0111_9lib_CAT	*smg-1* RNAi	H3K9me3 IP nucleosome	*rrf-3*(*pk1426*)	Chr. I:6,907,993–6,909,159 (*smg-1*)	13,550,730
SG0211_24lib	*smg-1* RNAi	H3K9me3 IP nucleosome	*rde-1*(*ne300*)	Chr. I:6,907,993–6,909,159 (*smg-1*)	13,212,520
SG0211_23lib	*smg-1* RNAi	H3K9me3 IP nucleosome	MAGO[b]	Chr. I:6,907,993–6,909,159 (*smg-1*)	14,629,944
AF_SOL_385	*smg-1* RNAi	Small RNA cloning	N2	Chr. I:6,907,993–6,909,159 (*smg-1*)	9,344,019
AF_SOL_388	*smg-1* RNAi	Small RNA cloning	MAGO[b]	Chr. I:6,907,993–6,909,159 (*smg-1*)	6,374,634
AF_SOL_389	*smg-1* RNAi	Small RNA cloning	*rde-1*(*ne300*)	Chr. I:6,907,993–6,909,159 (*smg-1*)	9,736,340
SG0511_lib1	*smg-1* RNAi	Small RNA cloning	*nrde-2*(*gg091*)	Chr. I:6,907,993–6,909,159 (*smg-1*)	9,594,600
SG0411_lib28	P_0 of multigenerational experiment	H3K9me3 IP nucleosome	N2	Chr. I:6,907,993–6,909,159 (*smg-1*)	6,665,856
SG0411_lib30	F_1 of multigenerational experiment	H3K9me3 IP nucleosome	N2		6,404,696
SG0411_lib32	F_2 of multigenerational experiment	H3K9me3 IP nucleosome	N2		7,192,377
SG0411_lib34	F_3 of multigenerational experiment	H3K9me3 IP nucleosome	N2		7,058,857
SG0411_lib14	24 h of *smg-1* RNAi feeding	H3K9me3 IP nucleosome	N2	Chr. I:6,907,993–6,909,159 (*smg-1*)	6,522,036
SG0411_lib16	4 h of *smg-1* RNAi feeding	H3K9me3 IP nucleosome	N2	Chr. I:6,907,993–6,909,159 (*smg-1*)	7,342,460
SG0511_lib9	F_1 of multigenerational experiment	Small RNA cloning	N2		5,994,713
SG0511_lib10	F_2 of multigenerational experiment	Small RNA cloning	N2		1,892,615
SG0511_lib11	F_3 of multigenerational experiment	Small RNA cloning	N2		4,591,831
SG0511_lib7	24 h of *smg-1* RNAi feeding	Small RNA cloning	N2	Chr. I:6,907,993-6,909,159 (*smg-1*)	5,111,519
SG0511_lib8	4 h of *smg-1* RNAi feeding	Small RNA cloning	N2	Chr. I:6,907,993-6,909,159 (*smg-1*)	3,823,974

[a]Number of reads that perfectly match the genome. [b]MAGO, combination of *ppw-1*(*tm914*), *sago-1*(*tm1195*), *sago-2*(*tm894*), *F58G1.1*(*tm1019*), *C06A1.4*(*tm887*) and *M03D4.6*(*tm1144*).

requires RdRP activity and, presumably, the resulting secondary siRNAs for alteration at the chromatin level.

Introns near the dsRNA trigger region show high H3K9me3 levels even though the siRNA levels are low. It is possible that the siRNA-associated chromatin modification enzymes act directly on sites that are somewhat spatially removed from an initial siRNA-transcript interaction. Alternatively, the observed spreading of the siRNA-induced signal may reflect an ability of H3K9me3 nucleosomes to recruit machinery that enforces new rounds of chromatin modification.

H3K9me3 is associated with repetitive DNA, centromeres and other DNA elements that need to be constitutively silenced. Our multigenerational analysis showed that dsRNA-triggered H3K9me3 could be passed on to subsequent generations, suggesting a possible basis for long-term control of mobile elements. Despite heritability of the altered chromatin state for several generations, we found that the chromatin at the target gene eventually reverted to the original (active) state in the absence of the trigger, which is consistent with the heritability of small RNAs being finite[55]. This observation suggests that truly heterochromatic states may need to be maintained by periodic production of an RNA trigger.

A working model for RNA-triggered chromatin modification is shown in **Figure 6**. Exogenous dsRNA is first processed by DICER complexes to produce primary siRNAs, which guide RDE-1 to its target mRNA. RdRP activities are then engaged to copy the target, yielding secondary siRNAs. Secondary siRNAs interact with a dedicated set of argonautes, including PPW-1, SAGO-1, SAGO-2 and F58G1.1. These interactions appear to be required for dsRNA-triggered H3K9 methylation. One possibility is that secondary siRNAs enter the nucleus directly, enforcing chromatin modification through interaction with either the nascent transcript or the DNA template. Alternatively, the siRNAs may be synthesized in the nucleus or may be 'handed off' in the cytoplasm to a shuttling argonaute, whose transport into the nucleus would then allow interaction with nascent RNA or DNA. The last model, albeit more complex, is supported by the requirement for NRDE-3 and for the corresponding cytoplasm-to-nucleus transport factor NRDE-2 for effective gene silencing in at least some cases[44,45]. Once a secondary siRNA–containing complex recognizes a chromatin-associated target (through basepairing with nascent transcripts or DNA), the next step would be the recruitment of a chromatin-modifying complex, producing a localized alteration in the histone code, including the methylation of H3K9 in nearby nucleosomes. The delayed time course of the chromatin response (compared with the fast siRNA response) suggests that the downstream components of this pathway (entry of small RNAs into the nucleus and/or modification of the histone code) may produce effects that are both slower and more stable than their mRNA-targeted RNAi counterparts.

METHODS

Methods and any associated references are available in the online version of the paper at http://www.nature.com/naturegenetics/.

Accession numbers. All sequencing data used in this study (**Table 1**) have been deposited in GEO (GSE32631).

ACKNOWLEDGMENTS

We thank Z. Weng, P. Lacroute, A. Sidow, H. Zhang, J. Merker, D. Wu, K. Artiles, L. Gracey, A. Lamm, C. Mello, M. Stadler, R. Alcazar and J. Ni for help, suggestions and support. Funding for this study was provided by a grant from the US National Institutes of Health (R01-GM37706).

AUTHOR CONTRIBUTIONS

Experiments were conceived in discussions among all authors. Experiments and data analyses for **Figure 1** were performed by S.G.G., J.P., J.M.M., S.G., S.K. and

A.F. Experiments and data analyses for **Figures 2–5** were performed by S.G.G., J.P. and A.F. Overall discussions of the data and implications involved all authors, and the manuscript was written by S.G.G. and A.F.

COMPETING FINANCIAL INTERESTS
The authors declare no competing financial interests.

Published online at http://www.nature.com/naturegenetics/.
Reprints and permissions information is available online at http://www.nature.com/reprints/index.html.

1. Fire, A. *et al.* Potent and specific genetic interference by double-stranded RNA in *Caenorhabditis elegans*. *Nature* **391**, 806–811 (1998).
2. Kennerdell, J.R. & Carthew, R.W. Use of dsRNA-mediated genetic interference to demonstrate that frizzled and frizzled 2 act in the wingless pathway. *Cell* **95**, 1017–1026 (1998).
3. Bernstein, E., Caudy, A.A., Hammond, S.M. & Hannon, G.J. Role for a bidentate ribonuclease in the initiation step of RNA interference. *Nature* **409**, 363–366 (2001).
4. Hammond, S.M., Boettcher, S., Caudy, A.A., Kobayashi, R. & Hannon, G.J. Argonaute2, a link between genetic and biochemical analyses of RNAi. *Science* **293**, 1146–1150 (2001).
5. Tuschl, T., Zamore, P.D., Lehmann, R., Bartel, D.P. & Sharp, P.A. Targeted mRNA degradation by double-stranded RNA *in vitro*. *Genes Dev.* **13**, 3191–3197 (1999).
6. Hammond, S.M., Bernstein, E., Beach, D. & Hannon, G.J. An RNA-directed nuclease mediates post-transcriptional gene silencing in *Drosophila* cells. *Nature* **404**, 293–296 (2000).
7. Elbashir, S.M., Lendeckel, W. & Tuschl, T. RNA interference is mediated by 21- and 22-nucleotide RNAs. *Genes Dev.* **15**, 188–200 (2001).
8. Motamedi, M.R. *et al.* Two RNAi complexes, RITS and RDRC, physically interact and localize to noncoding centromeric RNAs. *Cell* **119**, 789–802 (2004).
9. Pak, J. & Fire, A. Distinct populations of primary and secondary effectors during RNAi in *C. elegans*. *Science* **315**, 241–244 (2007).
10. Sijen, T., Steiner, F.A., Thijssen, K.L. & Plasterk, R.H. Secondary siRNAs result from unprimed RNA synthesis and form a distinct class. *Science* **315**, 244–247 (2007).
11. Saito, K. & Siomi, M.C. Small RNA-mediated quiescence of transposable elements in animals. *Dev. Cell* **19**, 687–697 (2010).
12. Claycomb, J.M. *et al.* The Argonaute CSR-1 and its 22G-RNA cofactors are required for holocentric chromosome segregation. *Cell* **139**, 123–134 (2009).
13. Batista, P.J. *et al.* PRG-1 and 21U-RNAs interact to form the piRNA complex required for fertility in *C. elegans*. *Mol. Cell* **31**, 67–78 (2008).
14. Gent, J.I. *et al.* Distinct phases of siRNA synthesis in an endogenous RNAi pathway in *C. elegans* soma. *Mol. Cell* **37**, 679–689 (2010).
15. Maniar, J.M. & Fire, A.Z. EGO-1, a *C. elegans* RdRP, modulates gene expression via production of mRNA-templated short antisense RNAs. *Curr. Biol.* **21**, 449–459 (2011).
16. Wassenegger, M., Heimes, S., Riedel, L. & Sanger, H.L. RNA-directed *de novo* methylation of genomic sequences in plants. *Cell* **76**, 567–576 (1994).
17. Matzke, M.A., Primig, M., Trnovsky, J. & Matzke, A.J. Reversible methylation and inactivation of marker genes in sequentially transformed tobacco plants. *EMBO J.* **8**, 643–649 (1989).
18. Wassenegger, M. RNA-directed DNA methylation. *Plant Mol. Biol.* **43**, 203–220 (2000).
19. Herr, A.J. & Baulcombe, D.C. RNA silencing pathways in plants. *Cold Spring Harb. Symp. Quant. Biol.* **69**, 363–370 (2004).
20. Volpe, T.A. *et al.* Regulation of heterochromatic silencing and histone H3 lysine-9 methylation by RNAi. *Science* **297**, 1833–1837 (2002).
21. Grewal, S.I. RNAi-dependent formation of heterochromatin and its diverse functions. *Curr. Opin. Genet. Dev.* **20**, 134–141 (2010).
22. Moazed, D. Small RNAs in transcriptional gene silencing and genome defence. *Nature* **457**, 413–420 (2009).
23. Mellone, B.G. *et al.* Centromere silencing and function in fission yeast is governed by the amino terminus of histone H3. *Curr. Biol.* **13**, 1748–1757 (2003).
24. Peters, A.H. *et al.* Partitioning and plasticity of repressive histone methylation states in mammalian chromatin. *Mol. Cell* **12**, 1577–1589 (2003).
25. Snowden, A.W., Gregory, P.D., Case, C.C. & Pabo, C.O. Gene-specific targeting of H3K9 methylation is sufficient for initiating repression *in vivo*. *Curr. Biol.* **12**, 2159–2166 (2002).
26. Bannister, A.J. *et al.* Selective recognition of methylated lysine 9 on histone H3 by the HP1 chromo domain. *Nature* **410**, 120–124 (2001).
27. Bühler, M., Verdel, A. & Moazed, D. Tethering RITS to a nascent transcript initiates RNAi- and heterochromatin-dependent gene silencing. *Cell* **125**, 873–886 (2006).
28. Simmer, F. *et al.* Hairpin RNA induces secondary small interfering RNA synthesis and silencing in *trans* in fission yeast. *EMBO Rep.* **11**, 112–118 (2010).
29. Simmer, F. *et al.* Loss of the putative RNA-directed RNA polymerase RRF-3 makes *C. elegans* hypersensitive to RNAi. *Curr. Biol.* **12**, 1317–1319 (2002).
30. Iida, T., Nakayama, J. & Moazed, D. siRNA-mediated heterochromatin establishment requires HP1 and is associated with antisense transcription. *Mol. Cell* **31**, 178–189 (2008).
31. Aronica, L. *et al.* Study of an RNA helicase implicates small RNA–noncoding RNA interactions in programmed DNA elimination in *Tetrahymena*. *Genes Dev.* **22**, 2228–2241 (2008).
32. Malone, C.D., Anderson, A.M., Motl, J.A., Rexer, C.H. & Chalker, D.L. Germ line transcripts are processed by a Dicer-like protein that is essential for developmentally programmed genome rearrangements of *Tetrahymena thermophila*. *Mol. Cell. Biol.* **25**, 9151–9164 (2005).
33. Nowacki, M. *et al.* RNA-mediated epigenetic programming of a genome-rearrangement pathway. *Nature* **451**, 153–158 (2008).
34. Pal-Bhadra, M. *et al.* Heterochromatic silencing and HP1 localization in *Drosophila* are dependent on the RNAi machinery. *Science* **303**, 669–672 (2004).
35. Deshpande, G., Calhoun, G. & Schedl, P. *Drosophila* argonaute-2 is required early in embryogenesis for the assembly of centric/centromeric heterochromatin, nuclear division, nuclear migration, and germ-cell formation. *Genes Dev.* **19**, 1680–1685 (2005).
36. Kanellopoulou, C. *et al.* Dicer-deficient mouse embryonic stem cells are defective in differentiation and centromeric silencing. *Genes Dev.* **19**, 489–501 (2005).
37. Taira, K. Induction of DNA methylation and gene silencing by short interfering RNAs in human cells (Retraction). *Nature* **441**, 1176 (2006).
38. Weinberg, M.S., Barichievy, S., Schaffer, L., Han, J. & Morris, K.V. An RNA targeted to the HIV-1 LTR promoter modulates indiscriminate off-target gene activation. *Nucleic Acids Res.* **35**, 7303–7312 (2007).
39. Morris, K.V., Chan, S.W., Jacobsen, S.E. & Looney, D.J. Small interfering RNA–induced transcriptional gene silencing in human cells. *Science* **305**, 1289–1292 (2004).
40. Kim, D.H., Villeneuve, L.M., Morris, K.V. & Rossi, J.J. Argonaute-1 directs siRNA-mediated transcriptional gene silencing in human cells. *Nat. Struct. Mol. Biol.* **13**, 793–797 (2006).
41. Weinberg, M.S. *et al.* The antisense strand of small interfering RNAs directs histone methylation and transcriptional gene silencing in human cells. *RNA* **12**, 256–262 (2006).
42. Timmons, L. & Fire, A. Specific interference by ingested dsRNA. *Nature* **395**, 854 (1998).
43. Tabara, H., Grishok, A. & Mello, C.C. RNAi in *C. elegans*: soaking in the genome sequence. *Science* **282**, 430–431 (1998).
44. Guang, S. *et al.* Small regulatory RNAs inhibit RNA polymerase II during the elongation phase of transcription. *Nature* **465**, 1097–1101 (2010).
45. Guang, S. *et al.* An Argonaute transports siRNAs from the cytoplasm to the nucleus. *Science* **321**, 537–541 (2008).
46. Montgomery, M.K., Xu, S. & Fire, A. RNA as a target of double-stranded RNA–mediated genetic interference in *Caenorhabditis elegans*. *Proc. Natl. Acad. Sci. USA* **95**, 15502–15507 (1998).
47. Grishok, A., Sinskey, J.L. & Sharp, P.A. Transcriptional silencing of a transgene by RNAi in the soma of *C. elegans*. *Genes Dev.* **19**, 683–696 (2005).
48. Gu, S.G. & Fire, A. Partitioning the *C. elegans* genome by nucleosome modification, occupancy, and positioning. *Chromosoma* **119**, 73–87 (2010).
49. Kennedy, S., Wang, D. & Ruvkun, G. A conserved siRNA-degrading RNase negatively regulates RNA interference in *C. elegans*. *Nature* **427**, 645–649 (2004).
50. Dufourcq, P. *et al. lir-2*, *lir-1* and *lin-26* encode a new class of zinc-finger proteins and are organized in two overlapping operons both in *Caenorhabditis elegans* and in *Caenorhabditis briggsae*. *Genetics* **152**, 221–235 (1999).
51. Smardon, A. *et al.* EGO-1 is related to RNA-directed RNA polymerase and functions in germ-line development and RNA interference in *C. elegans*. *Curr. Biol.* **10**, 169–178 (2000).
52. Hodgkin, J., Papp, A., Pulak, R., Ambros, V. & Anderson, P. A new kind of informational suppression in the nematode *Caenorhabditis elegans*. *Genetics* **123**, 301–313 (1989).
53. Brenner, S. The genetics of *Caenorhabditis elegans*. *Genetics* **77**, 71–94 (1974).
54. Sijen, T. *et al.* On the role of RNA amplification in dsRNA-triggered gene silencing. *Cell* **107**, 465–476 (2001).
55. Alcazar, R.M., Lin, R. & Fire, A.Z. Transmission dynamics of heritable silencing induced by double-stranded RNA in *Caenorhabditis elegans*. *Genetics* **180**, 1275–1288 (2008).
56. Yigit, E. *et al.* Analysis of the *C. elegans* Argonaute family reveals that distinct Argonautes act sequentially during RNAi. *Cell* **127**, 747–757 (2006).
57. Grishok, A., Tabara, H. & Mello, C.C. Genetic requirements for inheritance of RNAi in *C. elegans*. *Science* **287**, 2494–2497 (2000).
58. Vastenhouw, N.L. *et al.* Gene expression: long-term gene silencing by RNAi. *Nature* **442**, 882 (2006).
59. Hamilton, A.J. & Baulcombe, D.C. A species of small antisense RNA in posttranscriptional gene silencing in plants. *Science* **286**, 950–952 (1999).
60. Dalmay, T., Hamilton, A., Rudd, S., Angell, S. & Baulcombe, D.C. An RNA-dependent RNA polymerase gene in *Arabidopsis* is required for posttranscriptional gene silencing mediated by a transgene but not by a virus. *Cell* **101**, 543–553 (2000).
61. Mourrain, P. *et al. Arabidopsis SGS2* and *SGS3* genes are required for posttranscriptional gene silencing and natural virus resistance. *Cell* **101**, 533–542 (2000).
62. Tabara, H., Yigit, E., Siomi, H. & Mello, C.C. The dsRNA binding protein RDE-4 interacts with RDE-1, DCR-1, and a DExH-box helicase to direct RNAi in *C. elegans*. *Cell* **109**, 861–871 (2002).
63. Tabara, H. *et al.* The *rde-1* gene, RNA interference, and transposon silencing in *C. elegans*. *Cell* **99**, 123–132 (1999).

ONLINE METHODS

***C. elegans* mutant strains used in this study.** *C. elegans* strain N2 (ref. 53) was used as the standard wild-type strain. Mutant alleles used in this study were *eri-1* (*mg366*)[49], *rde-1*(*ne300*)[63], *rrf-3*(*pk1426*)[54], *nrde-2*(*gg091*)[44], MAGO (*ppw-1* (*tm914*), *sago-1*(*tm1195*), *sago-2*(*tm894*), *F58G1.1*(*tm1019*), *C06A1.4*(*tm887*) and *M03D4.6*(*tm1144*))[56], *glp-1*(*e2141*)[64] and *glp-4*(*bn2*)[65]. All genomic coordinates are relative to version WS190 (WormBase[66]).

RNAi. RNAi by feeding was carried out as previously described[42]. The initial *smg-1* RNAi vector (chr. I: 6,907,993–6,909,159) was from the Cambridge RNAi library[67]. Other RNAi vectors used in this study were prepared in vector L4440 (ref. 68). The relevant target positions are chr. X: 15,728,059–15,728,991 (*lin-15B*), chr. II: 7,680,827–7,682,011 (*lir-1*), chr. I: 7,654,481–7,655,024 (*ego-1*), chr. I: 6,901,030–6,901,541 (*smg-1*, 3′ end) and chr. I: 6,913,664–6,913,933 (*smg-1*, 5′ end).

Multigenerational analysis of RNAi response. Wild-type adult animals were raised on bacteria producing dsRNA for *smg-1* for 2–3 generations, and this was followed by bleaching to produce a synchronized population[53] and continued culture on *smg-1* dsRNA bacteria. Adult animals from this population (designated as the P_0 generation for this experiment) were collected and divided into two groups: one was used for the siRNA and H3K9me3 profiling and the other was bleached to produce progeny designated as the F_1 generation. The bleaching also served to destroy bacteria expressing the dsRNA, allowing dsRNA triggering to be discontinued in the F_1 animals, which were fed on OP50 *Escherichia coli* lacking a dsRNA-producing plasmid. F_2 and F_3 animals were similarly raised on OP50 *E. coli*. Populations of F_1, F_2 and F_3 animals were then collected as adults for siRNA and H3K9me3 profiling.

H3K9me3 nucleosome immunoprecipitation. Frozen embryo pellets (50–100 µl) or frozen adult worm pellets (100–200 µl) were used for each nucleosome immunoprecipitation experiment. Crushed pellets (pulverized by grinding in liquid nitrogen with a mortar and pestle) were resuspended in 1 ml of buffer A (15 mM Hepes-Na, pH 7.5, 60 mM KCl, 15 mM NaCl, 0.15 mM β-mercaptoethonal, 0.15 mM spermine, 0.15 mM spermidine, 0.34 M sucrose and 1× HALT protease and phosphatase inhibitor cocktail (ThermoScientific)). To cross-link, we added formaldehyde to the resulting crude extract to a final concentration of 2% and then incubated samples at room temperature for 15 min. Then, 0.1 ml of 1 M Tris-HCl (pH 7.5) was added to quench formaldehyde. Lysates were spun (15,000 g for 1 min) and were washed with ice-cold buffer A and then resuspended in 0.3 ml of buffer A with 2 mM $CaCl_2$. Micrococcal nuclease (Roche) was added to the lysate to a final concentration of 0.3 U/µl, and samples were incubated at 37 °C for 5 min (inverting the tube several times per minute). Micrococcal nuclease (MNase) digestion was optimized so that approximately 70% of DNA entered the mono-nucleosome band, with the remainder predominantly in di- and trinucleosome bands. Digestion reactions were stopped by adding EGTA to a final concentration of 20 mM. After centrifugation (15,000*g* for 1 min), pellets were washed with ice-cold RIPA buffer (1× PBS, 1% NP40, 0.5% sodium deoxycholate, 0.1% SDS, 1× HALT protease and phophatase inhibitor and 2 mM EGTA), resuspended in 0.8 ml of ice-cold RIPA buffer and solubilized by sonication (Microson TM XL 2000 sonicating machine with a microtip, output level: 5, three repeats of a 30-s sonication). Sonication was used here to efficiently solubilize cross-linked chromatin without further fragmenting the chromatin (data not shown). Crude lysate was cleared by centrifugation at 15,000*g* for 2 min. An aliquot (80 µl) of the supernatant was used to make IP input nucleosome libraries. The remaining supernatant was used for immunoprecipitation, and we added 2 µg of antibody to H3K9me3 (ab8898, Abcam) and agitated gently at 4 °C overnight. Then, 50 µl of protein A Dynabeads (10% slurry in 1× PBS) was added and the resulting mixture shaken for 2 h at 4 °C. The beads were then washed four times (4 min per wash) with 600 µl of ice-cold LiCl washing buffer (100 mM Tris-HCl, pH 7.5, 500 mM LiCl, 1% NP-40 and 1% sodium deoxycholate), with samples being transferred to a new tube after the first wash. To elute the immunoprecipitated nucleosome and reverse cross-links, beads were incubated with 450 µl of worm lysis buffer (0.1 M Tris-HCl, pH 8.5, 100 mM NaCl and 1% SDS) containing 200 µg/ml of proteinase K at 65 °C for 4 h with agitation every 30 min (total nucleosome aliquots were treated similarly to reverse cross-link samples) and then subjected to organic extraction and DNA precipitation. DNA libraries were prepared as previously described[48], with the following change: immunoprecipitated or input DNA was used for end processing linker ligation without size selection. Linkered DNA corresponding to the nucleosome cores was size selected on a 6% denaturing PAGE gel (8 M urea).

High-throughput DNA sequencing and data analysis. DNA libraries were sequenced using an Illumina Gene Analyzer IIx. After removing barcodes, 25-nt reads were aligned to the *C. elegans* genome (SW190) using Bowtie[69] (see **Table 1** for more detailed experimental description). Only perfect alignments were used for analysis. Nucleosome cores were modeled as 147 bases of sequences extending from the first base of alignment. Nucleosome coverage at any given position was calculated by dividing the number of nucleosome cores that cover this position by the number of total alignments (in millions). If a read matched multiple positions in the genome, a fraction (1/the number of matches) was used to calculate nucleosome coverage.

Small RNA capture and sequencing. Small RNAs were captured using a 5′-monophosphate–independent method[70] (see **Table 1** for more detailed experimental description). To obtain a provisional measure of primary siRNA levels, we doubled the count of sense-stranded siRNAs in the trigger region, avoiding ambiguity in assigning antisense siRNAs in the trigger region by doubling the sense counts. A measure of secondary siRNAs from a given trigger region was then obtained by subtracting half of the presumed primary siRNA counts from total siRNAs on the antisense strand.

64. Austin, J. & Kimble, J. *glp-1* is required in the germ line for regulation of the decision between mitosis and meiosis in *C. elegans*. *Cell* **51**, 589–599 (1987).
65. Beanan, M.J. & Strome, S. Characterization of a germ-line proliferation mutation in *C. elegans*. *Development* **116**, 755–766 (1992).
66. Harris, T.W. *et al.* WormBase: a comprehensive resource for nematode research. *Nucleic Acids Res.* **38**, D463–D467 (2010).
67. Kamath, R.S. *et al.* Systematic functional analysis of the *Caenorhabditis elegans* genome using RNAi. *Nature* **421**, 231–237 (2003).
68. Timmons, L., Court, D.L. & Fire, A. Ingestion of bacterially expressed dsRNAs can produce specific and potent genetic interference in *Caenorhabditis elegans*. *Gene* **263**, 103–112 (2001).
69. Langmead, B., Trapnell, C., Pop, M. & Salzberg, S.L. Ultrafast and memory-efficient alignment of short DNA sequences to the human genome. *Genome Biol.* **10**, R25 (2009).
70. Gent, J.I. *et al.* A *Caenorhabditis elegans* RNA-directed RNA polymerase in sperm development and endogenous RNA interference. *Genetics* **183**, 1297–1314 (2009).